Title: Examination of the effect of selected factors on the photovoltaic response of dye-sensitized solar cells

Author: Paweł Gnida, Marcin Libera, Agnieszka Pająk, Ewa Schab-Balcerzak

Citation style: Gnida Paweł, Libera Marcin, Pająk Agnieszka, Schab-Balcerzak Ewa. (2020). Examination of the effect of selected factors on the photovoltaic response of dye-sensitized solar cells. "Energy and Fuels" (2020, iss. 11, s. 14344-14355), DOI:10.1021/acs.energyfuels.0c02188

energy&fuels

pubs.acs.org/EF Article

Examination of the Effect of Selected Factors on the Photovoltaic Response of Dye-Sensitized Solar Cells

Paweł Gnida, Marcin Libera, Agnieszka Pająk, and Ewa Schab-Balcerzak*

Cite This: *Energy Fuels* 2020, 34, 14344−14355

Read Online

ACCESS | Metrics & More | Article Recommendations

ABSTRACT: The impact of photoanode preparation on the photovoltaic performance of dye-sensitized solar cells was investigated. The effects of titanium dioxide layer thickness, type of solvent and immersion time used for photoanode fabrication, and addition of coadsorbents and a cosensitizer on photon-to-current conversion efficiency and photovoltaic parameters were studied. Commercially available N719 and dyes prepared in our research group, 5,5′-bis(2-cyano-1-acrylic acid)-2,2′-bithiophene and 2-cyano-3-(2,2′:5′,2″-terthiophen-5-yl)acrylic acid, were applied as sensitizers. The effect of studied factors on UV−vis properties and morphology, that is, the root-mean-square roughness of the photoanode, was examined and correlated with the photovoltaic response of the constructed devices. Additionally, the amount of dye molecules adsorbed to the TiO_2 was investigated. It was found that all considered factors significantly impacted photovoltaic parameters. Also, the photoanode stability was tested by measuring photovoltaic parameters after 14 months.

1. INTRODUCTION

The constantly growing demand for electricity and challenges with environmental pollution that lasts for years oblige the research for renewable energy sources that could replace fossil fuels. Photovoltaics, among which are dye-sensitized solar cells (DSSCs), have been intensively developed.[1,2] The most commonly used commercial dyes (sensitizers) are Ru complexes (N3, N719, or N749). The devices containing dyes based on ruthenium are characterized by good optical properties in the UV−vis range and high photovoltaic performance. The effect of solar cell preparation methods on photovoltaic parameters can be demonstrated by using the example of DSSCs containing N719 dye, which achieved efficiencies in the range of 1.9%−8.7%.[3−6] Dye cells first constructed in 1991 became popular around the year 2000, when they reached an efficiency above 10%.[7] The most important and interesting advantages of dye-sensitized solar cells can be summarized as follows: simple and low-cost manufacturing, low toxicity, and good performance in varied light conditions.[8] Due to their simple construction, DSSCs can significantly reduce the cost of solar energy. The dye-sensitized type of solar cell has a sandwich structure consisting of a glass substrate covered by a transparent, conductive layer (e.g., tin oxide, TCO), a semiconductor metal oxide layer (e.g., titanium dioxide or zinc oxide), an anchored dye, and a counter electrode, usually a nanoplatin deposited onto TCO.[9,10] The volume between electrodes has to be perfused by an electrolyte, for example, the I^-/I_3^- or Co^{2+}/Co^{3+} redox pair. Each of the constructive elements has a significant influence on the final performance of devices, and researches concerning new dyes, electrolytes, and electrodes are being carried out.[11−18] Moreover, the DSSC preparation parameters impact the photovoltaic performance, and such investigations can be found in the literature. Therein, the influence of solvent type;[19] thickness and nanocrystalline structure;[20−23] coadsorbent addition;[24−28] and additives to the semiconductor layer, such as sophisticated nanostructured oxides (e.g., nanowires, nanorods or nanoflowers) or nanoparticles of alternative oxides (e.g., ZnO)[29−36] or mixtures of dyes, among others, is presented.[37−39] The vast majority of the studies were focused on materials that make up solar cells, excluding dyes, that is, photoanode (preparation methods and materials), electrolyte (type of liquid or solid), and counter electrode (materials).[8,40] The enhancement of DSSC performance by improving the constructive elements, especially the photoanode, has been intensively investigated, as found in a literature overview. The impact of more than one parameter on the performance of DSSCs is still thinly discussed in the literature, nevertheless.

Herein, the results of research concerning the influence of photoanode preparation on the efficiency of DSSCs are presented. The process of cell preparation was optimized in terms of the selection of semiconductor TiO_2 layer thickness, solvent type, and immersion time in the dye solution. The effect of mixing of dyes and coadsorbents on photovoltaic parameters was tested as well. Additionally, the impact of photoanode preparation on its optical properties and root-mean square (RMS) roughness was investigated and correlated with the efficiency of the fabricated devices. The commercially available dye ruthenium(II)(2,2′-bipyridyl-4,4′-dicarboxylic acid)(2,2′-bipyridyl-4,4′-ditetrabutylammonium carboxylate)-

Received: July 1, 2020
Revised: September 23, 2020
Published: September 29, 2020

https://dx.doi.org/10.1021/acs.energyfuels.0c02188
Energy Fuels 2020, 34, 14344−14355

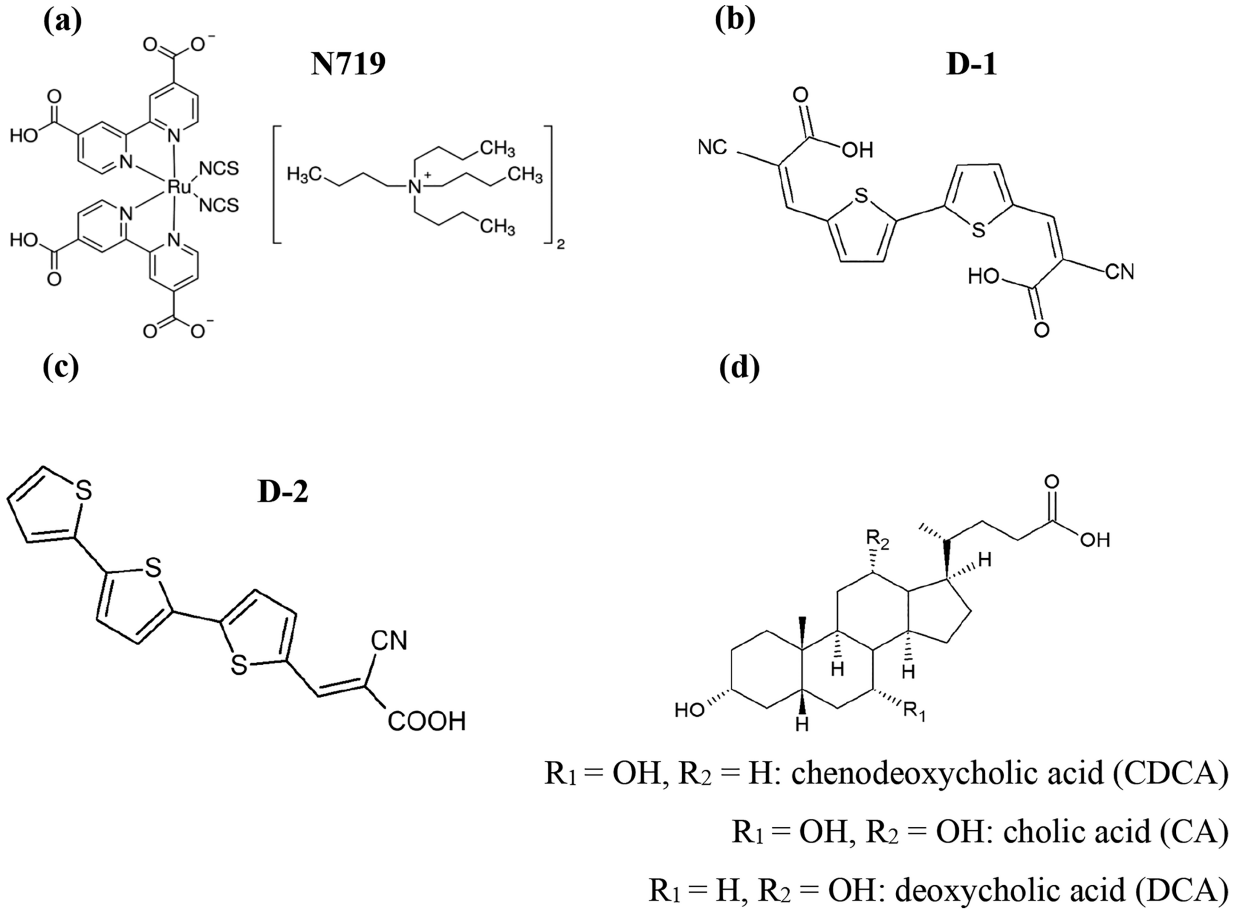

Figure 1. Chemical structure of the used dyes: (a) ruthenium metal complex N719, (b) 5,5′-bis(2-cyano-1-acrylic acid)-2,2′-bithiophene (D-1), (c) 2-cyano-3-(2,2′:5′,2″-terthiophen-5-yl)acrylic acid (D-2), and (d) coadsorbents.

$(NCS)_2$, denoted as N719, and compounds 5,5′-bis(2-cyano-1-acrylic acid)-2,2′-bithiophene (D-1) and 2-cyano-3-(2,2′:5′,2″-terthiophen-5-yl)acrylic acid (D-2), reported in our previous work,[41] were applied as sensitizers.

2. EXPERIMENTAL SECTION

2.1. Materials. Fluorine-doped tin oxide coated glass slides (FTOs, 7 Ω/sq, Sigma-Aldrich), 18NR-T titania paste (Greatcell Solar Materials), surfactant (Hellmanex III, Hellma Analytics), 2-propanol (IPA) (POCH), ruthenium(II)(2,2′-bipyridyl-4,4′-dicarboxylic acid)(2,2′-bipyridyl-4,4′-ditetrabutylammonium carboxylate)-$(NCS)_2$ (N719), and EL-HSE electrolyte were purchased from Sigma-Aldrich. 5,5′-Bis(2-cyano-1-acrylic acid)-2,2′-bithiophene and 2-cyano-3-(2,2′:5′,2″-terthiophen-5-yl)acrylic acid were prepared as reported in ref 41. Methanol (Avantor Performance Materials), *N*,*N*-dimethylformamide (Aldrich), *tert*-butyl alcohol (*t*-BuOH) (Chempur), acetonitrile (Sigma), cholic acid (Sigma), deoxycholic acid (Sigma), and chenodeoxycholic acid (Sigma) were used in device preparation.

2.2. Measurements. The UV−vis absorptions spectra of TiO_2 with adsorbed N719 were recorded using a V-570 UV−vis−NIR spectrophotometer (Jasco Inc.). XRD patterns were registered using a Bruker D8 Advance. The nanoscale morphology of the surface of electrodes was characterized by atomic force microscopy (AFM) using a TopoMetrix Explorer device, operating in contact mode, in air, in the constant force regime. The thickness and morphology in the broad range of TiO_2 layers were determined using an optical microscope (OLYMPUS DSX500i). The cross-sectional SEM images were taken using a SEM microscope (Quanta/FEG 250/FEI Co.). The incident photon-to-current efficiency (IPCE) spectra were registered by a photoelectric spectrometer using a xenon lamp (Ushio UXL-151H 150 W, Photonic Institute). The devices were tested using a PV Solutions solar simulator and a Keithley 2400 SourceMeter (Tektronix, Inc., Beaverton, OR) under AM 1.5 G illumination (100 mW cm^{-2}).

2.3. Dye-Loading Analysis. The amount of dye adsorbed on TiO_2 was estimated by adsorption−desorption studies performed according to the literature methods.[42,43] At the beginning, solutions of N719 in 10 mM NaOH with different concentrations of dye were prepared and the UV−vis absorption spectra were recorded. On the basis of recorded UV−vis spectra, a calibration curve for N719 was prepared. Further, sensitized TiO_2 substrates were immersed in 10 mM NaOH solution for 2 h. During this time, the dye molecules desorbed from the TiO_2 films, which was confirmed by the absorption spectra of the substrates. Then, the absorbance of the dye in the NaOH solution was measured by UV−vis absorption spectroscopy. The volume of solutions was 5 mL and in each case was identical. On the basis of the absorption maxima of the solution obtained and the prepared reference solutions, the dye loading was calculated from a calibration curve.

2.4. Procedure of Photoanode Preparation. All FTOs slides were cleaned before use as follows. The FTOs (2 × 2 cm^2) were washed in a mixture of deionized water and Hellamanex (9:1 by vol) for 5 min and then rinsed twice with hot distilled water (50 mL). Such slides were ultrasonicated in IPA for 5 min and rinsed twice with hot distilled water (50 mL). After washing, FTOs were dried in hot air. A TiO_2 layer was screen-printed on cleaned FTO and dried at 125 °C for 5 min and cooled down. In the same way, other TiO_2 layers were screen-printed until an adequate number of layers was obtained. Next, FTO slides with an adequate number of TiO_2 layers (from one to four) were fired at 500 °C in air for 30 min. FTOs covered by TiO_2 were immersed in a N719 solution (c = 3 × 10^{-4} M) of the

https://dx.doi.org/10.1021/acs.energyfuels.0c02188
Energy Fuels 2020, 34, 14344−14355

appropriate solvent (in DMF, MeOH, or ACN:*t*-BuOH). After a specified time, the excess of a dye was flush away by MeOH. The prepared photoanodes with adsorbed dye molecules were employ to assembly a sandwich-structured solar cell (FTO/TiO_2+dye/EL-HSE/Pt/FTO) by fixing it to a counter electrode (Pt/FTO). The electrolyte consists of the iodide/triiodide redox couple that was injected between the electrodes.

3. RESULTS AND DISCUSSION

The impact of various factors of photoanode fabrication—the thickness of the TiO_2 (number of TiO_2 layers), solvent type used for dye solution preparation, immersion time of electrode in sensitizer solution, and coadsorbents addition—on the UV−vis absorption properties, the roughness of the electrode, the IPCE, and, finally, the photovoltaic (PV) characteristics of DSSC cells with the structure FTO/TiO_2+dye/EL-HSE electrolyte/Pt/FTO was investigated. Additionally, the effect of the dye mixtures utilized was presented. The chemical structures of the applied dyes and coadsorbents are depicted in Figure 1.

3.1. Effect of TiO_2 Thickness. The thickness of the TiO_2 layer was the first considered factor affecting the morphology and optical properties of the photoanode and finally the PV response. It is generally understood that the thickness of the TiO_2 depends on the number of screen-printed oxide layers. Anodes consisting of one, two, three, and four TiO_2 layers were prepared. Next, the electrodes were immersed in a solution of N719 dissolved in a mixture of acetonitrile and *t*-BuOH (1:1) ($c = 3 \times 10^{-4}$ M) for 48 h. The thickness of the TiO_2 with adsorbed N719 was determined using an optical microscope. It was determined that the thickness of the semiconducting oxide consisting of one, two, three, and four TiO_2 layers was 4.5, 7.3, 8.4, and 15 μm, respectively (cf. Table 1). Additionally, the thickness of the TiO_2 was measured by a scanning electron microscope (SEM), and the cross-sectional SEM images of devices with four, three, and two semiconducting oxide layers are given in Figure 2f−h. The thicknesses estimated from optical microscopy agree well with those obtained from SEM measurements.

Table 1. Thickness and Roughness Parameters of Surfaces of Multiple TiO_2 Layers Screen-Printed on FTOs

			optical microscopy		
no. of TiO_2 layers		AFM: RMS roughness(nm)	thickness (μm)	Sq (μm)[a]	Sku[b]
1	with N719	27	4.5	0.211	5.774
	without dye	36			
2	with N719	35	7.3	0.211	5.774
	without dye	45			
3	with N719	53	8.4	0.111	8.643
	without dye	68			
4	with N719	65	15	0.214	7.166
	without dye	86			

[a]Root-mean-square height. [b]Sharpness of the roughness profile.

The surface morphology, especially the roughness of the electrode, as an important factor concerning the performance of the DSSC, was examined using optical and atomic force microscopies. The morphology of electrode surfaces consisting of one, two, three, and four TiO_2 layers is presented in Figure 2.

The roughness value of the broad range of surfaces was measured for an area as a root-mean-square height (Sq) as well as via a sharpness of the roughness profile (Sku). The results for surfaces after multiple screen-printing of TiO_2 are presented in Table 1. The roughness, as well sharpness, after one and two layers of screen-printing is equal. The roughness (Sq) does not increases significantly in the case of four layers, but the sharpness is considerably higher. However, all of the layers are characterized by the same type of sharpness (Figure 2e). The measurements of the nanoscale root-mean-square (RMS) roughness executed by AFM indicate that substrates with and without dye were not quite planar in the nanorange of area (cf. Table 1). Figure 3 shows AFM micrographs of substrates consisting of one and four TiO_2 layers without and with dye.

Together with the increase of TiO_2 number layers, an increase of the RMS roughness was observed. The photoanodes covered by dye molecules were characterized by lower RMS roughness values than substrates without adsorbed dye.

Before focusing on the PV response of devices with different TiO_2 thicknesses, it is important to discuss the UV−vis absorption properties of photoanodes, which are crucial to the PV performance. Hence, the absorption spectra of photoanodes were recorded and are depicted in Figure 4a.

As can be concluded on the basis of Figure 4a, the thickness of the titanium dioxide significantly impacts the light absorption ability. The absorption intensity of the photoanode gradually rises upon increasing the TiO_2 layer number from one to three. However, in the case of four TiO_2 layers, the absorption intensity decreased. Reduction of absorption may be caused by excessive thickness of the TiO_2 layer, which may constitute a physical blockade for light before it reaches the dye molecules.[44] The photoanode consisting of three TiO_2 layers exhibited the most intense absorption band compare to the others. Thus, the electrode that consisted of three TiO_2 layers with a thickness of 8.4 μm was examined using X-ray measurements, and the XRD pattern is shown in Figure 4b. The main peak was located at $2\theta = 25.28°$. The peaks disclosed at 2θ values of 25.30°, 36.94°, 37.79°, 38.57°, 48.04°, 53.87°, and 55.06° (Crystallography Open Database) confirm the anatase structure. The obtained results are consistent with those reported in the literature, which indicate the formation of an anatase crystalline structure after utilization of 500 °C as the annealing temperature of TiO_2.[20,23] It was found that solar cells with the anatase crystalline structure of TiO_2 exhibited better photovoltaic performance, probably due to the fact that the anatase form is characterized by a larger specific surface area, porosity, and number of hydroxyl surface groups than the rutile structure. The average reported crystal size of anatase is 150 Å.[45]

In the next step of the investigation, the devices differing in TiO_2 thickness were fabricated and the IPCE was measured. IPCE spectra exhibited a broad band in the region of 350−750 nm with a maximum value at about 500 nm. The IPCE maximum is red-shifted by 40 nm relative to the maximum absorption peak wavelength. The IPCE curves show that the low-energy electrons could be more effectively transmitted to the conduction band of TiO_2. From these results, it is seen that devices with TiO_2 thicknesses of 7.3 and 8.4 μm showed

https://dx.doi.org/10.1021/acs.energyfuels.0c02188
Energy Fuels 2020, 34, 14344−14355

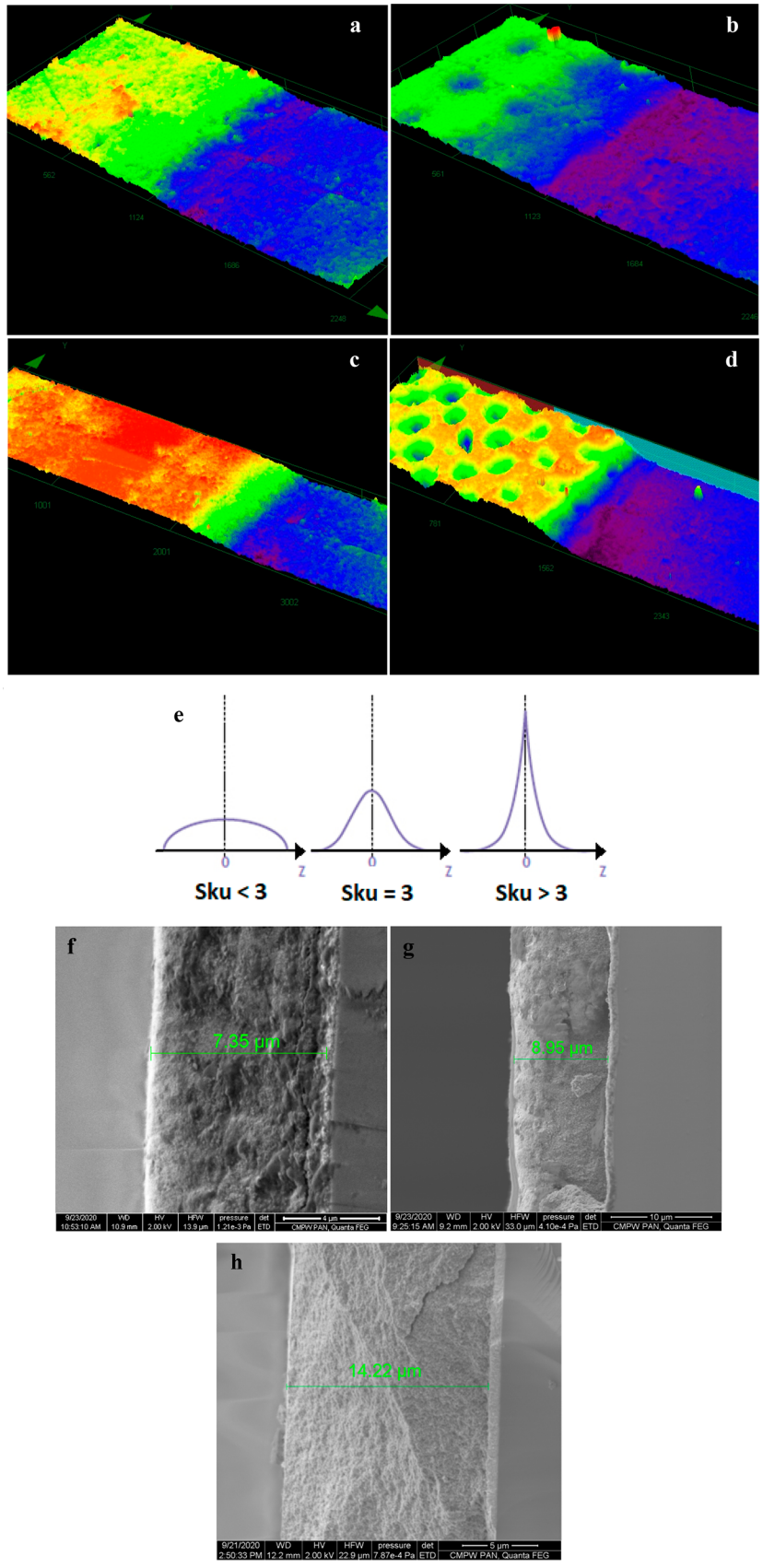

Figure 2. Micrographs of electrodes with (a) one, (b) two, (c) three, and (d) four TiO_2 layers. (e) Sharpness of roughness profile type depending on Sku value for three TiO_2 layers. Cross-sectional SEM images of devices differing in the number of TiO_2 layers: (f) two, (g) three, and (h) four.

https://dx.doi.org/10.1021/acs.energyfuels.0c02188
Energy Fuels 2020, 34, 14344−14355

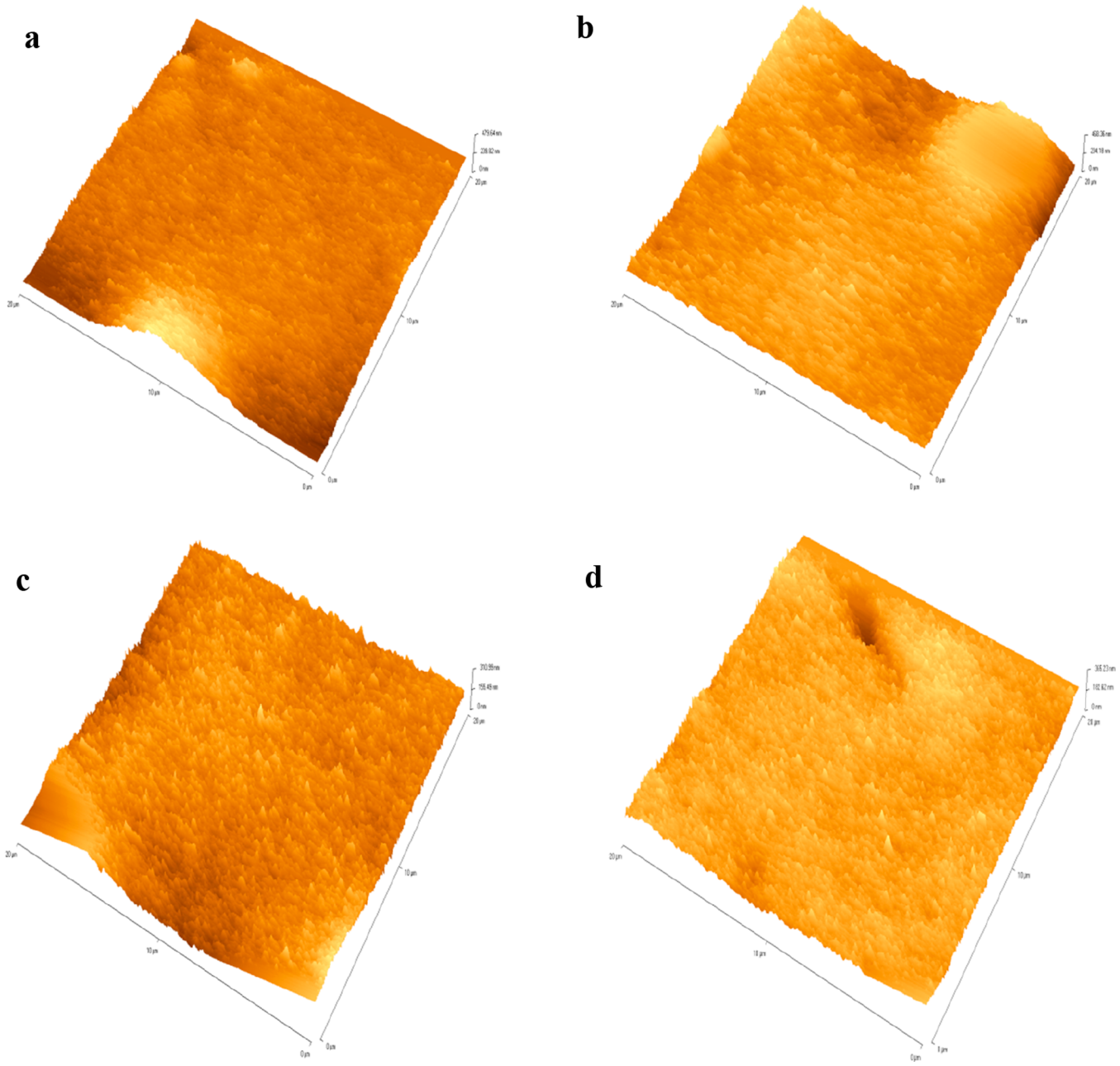

Figure 3. AFM micrographs of electrodes consisting of (a) one TiO_2 layer without N719, (b) one TiO_2 layer with N719, (c) four TiO_2 layers without N719, and (d) four TiO_2 layers with N719.

similar IPCE maximum values of 33% and 32%, while the cell with four TiO_2 layers exhibited a less intense band (cf. Table 2). The photovoltaic parameters [open-circuit voltage (V_{oc}), short-circuit current density (J_{sc}), fill factor (FF), and photovoltaic efficiency (PCE)] of DSSCs calculated from photocurrent density−voltage ($J-V$) curves are summarized in Table 2. Additionally, photocurrent densities ($J_{sc\text{-}IPCE}$) were calculated from IPCE spectra. The obtained $J-V$ curves are depicted in Figure 5.

The highest conversion efficiency was obtained for the solar cell containing three TiO_2 layers (8.4 μm). The J_{sc} values obtained from $J-V$ measurements correspond to the J_{sc} calculated from IPCE spectra ($J_{sc\text{-}IPCE}$).[46] However, small differences in the PCE values of devices containing of two, three, and four TiO_2 layers are observed. Application of a lower number of TiO_2 layers is important from an economical point of view of photoanode preparation. The decrease in the efficiency of the device with the thickest TiO_2 layer is due to the decrease in photocurrent density. The evidence described in the literature indicates the variability of the maximum efficiency depending on the thickness of the TiO_2 layer. In the reported case of DSSCs with a TiO_2 layer thickness in the range of 8−32 μm also sensitized with N719, the highest PCE (3.43%) was obtained for the device with a 24 μm layer.[47] Other work revealed that the most efficient DSSCs contained TiO_2 with a thickness between 3.5 and 14 μm,[48] and the highest PCE (5.93%) was obtained for a cell with a 10 μm TiO_2 layer.

Further, the desorption study revealed that the amount of adsorbed dye, given in Table 2, does not correlate very well

https://dx.doi.org/10.1021/acs.energyfuels.0c02188
Energy Fuels 2020, 34, 14344−14355

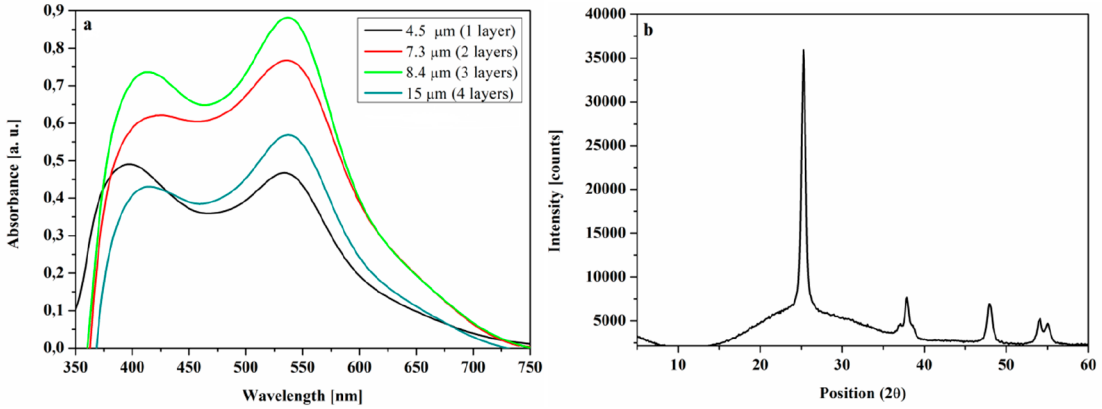

Figure 4. (a) UV−vis spectra of photoanodes based on N719 with different TiO_2 layer numbers and (b) XRD pattern of an electrode consisting of three TiO_2 layers annealed at 500 °C.

Table 2. Photovoltaic Parameters of Cells with the Structure FTO/TiO_2+N719/EL-HSE Electrolyte/Pt/FTO Collected from *J*−*V* Curves and IPCE Spectra

TiO_2 thickness (μm)	V_{oc} (mV)	J_{sc} (mA cm^{-2})	FF	PCE (%)	IPCE$_{max}$ (%)	$J_{sc\text{-}IPCE}$ (mA cm^{-2})	dye loading (mol cm^{-2})
4.5	689	13.66	0.44	4.20			2.63×10^{-7}
7.3	720	17.42	0.44	5.75	33	12.14	2.70×10^{-7}
8.4	762	14.34	0.54	5.99	32	12.62	2.84×10^{-7}
15.0	733	13.60	0.57	5.80	16	11.33	3.02×10^{-7}

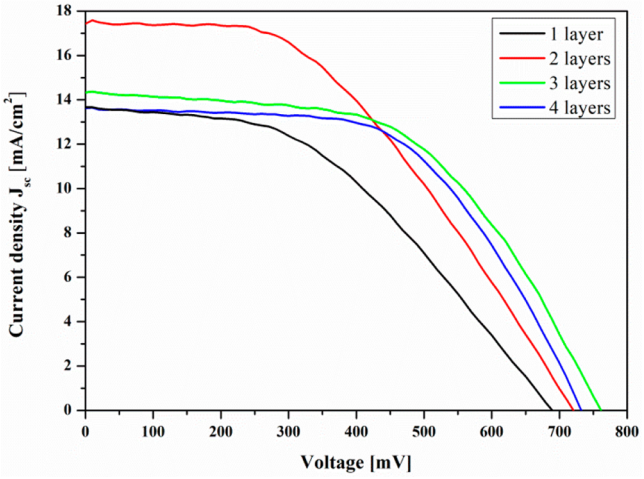

Figure 5. Photocurrent density−voltage curves (*J*−*V*) of DSSCs differing in TiO_2 thickness (immersion time 48 h in ACN:*t*-BuOH dye solutions).

with the current density values of the fabricated solar cells. The highest amount of absorbed dye (3.02×10^{-7}) did not translate into the total efficiency of the device, probably due to the previously mentioned excessive thickness of the TiO_2 layer.[44]

Summarizing, from the presented results it can be concluded that the anodes consisting of three or two TiO_2 layers seem to be the most promising for DSSC preparation. Therefore, for the next step of investigations, such anodes were applied.

3.2. Effect of Solvent Type and Immersion Time. The solvent type and immersion time of the anode in the dye solution were the next investigated factors influencing the PV performance of DSSCs. It is worth noting that in the literature there is a lack of data concerning the effect of the solvent type used for anode dye sensitization on the PV parameters of DSSC devices. Usually, the impact of solvent on the electrolyte action is examined.[19,49,50]

The dye solutions based on N719 were prepared using MeOH, DMF, or ACN:*t*-BuOH (1:1) with a concentration of 3×10^{-4} M. The photoanodes were immersed in the dye solution for 24, 48, and 72 h. The UV−vis absorption spectra of TiO_2 substrate with adsorbed N719 prepared in different solvents were collected and are presented in Figure 6a. The adsorption of dye molecules onto the surface is closely relating to the solvents applied to prepare the dye solution.

The results indicate that a more intense absorption band was a characteristic of a photoanode prepared from ACN:*t*-BuOH. Moreover, in most cases, a longer immersion time improves the absorbance of the photoanode (cf. Figure 6b) and PV parameters of the device. However, in the literature, there are reports that showed that increasing the immersion time does not always cause an increase in the PV response.[34,51−53]

From the IPCE spectra, given in Figure 7, it is seen that the IPCE curve of the cell with its photoanode prepared in a mixture of solvents shows a broad band in the region of 350−700 nm with a maximum value at 470 nm, while devices with their photoanode fabricated in MeOH and DMF exhibit less intense bands, especially in the region of 350−470 nm. The lowest IPCE values were recorded for DSSCs prepared from MeOH and DMF solutions, being in agreement with the UV−vis spectra (cf. Table 3). The observed differences can be due to a higher adsorption of dye to the TiO_2 surface in ACN:*t*-BuOH, i.e., 2.95×10^{-7} mol cm^{-2}, in comparison with the other solvents (Table 3). The better IPCE response of the device with its photoanode obtained in ACN:*t*-BuOH can be interpreted in terms of a higher J_{sc} value leading to an improved PCE value (cf. Table 3).

Taking into account the same immersion time of the anode in various dye solutions, the PCE value was found to be in the order ACN:*t*-BuOH > DMF > MeOH. The observed solvent effect can be explained by considering the donor−acceptor

https://dx.doi.org/10.1021/acs.energyfuels.0c02188
Energy Fuels 2020, 34, 14344−14355

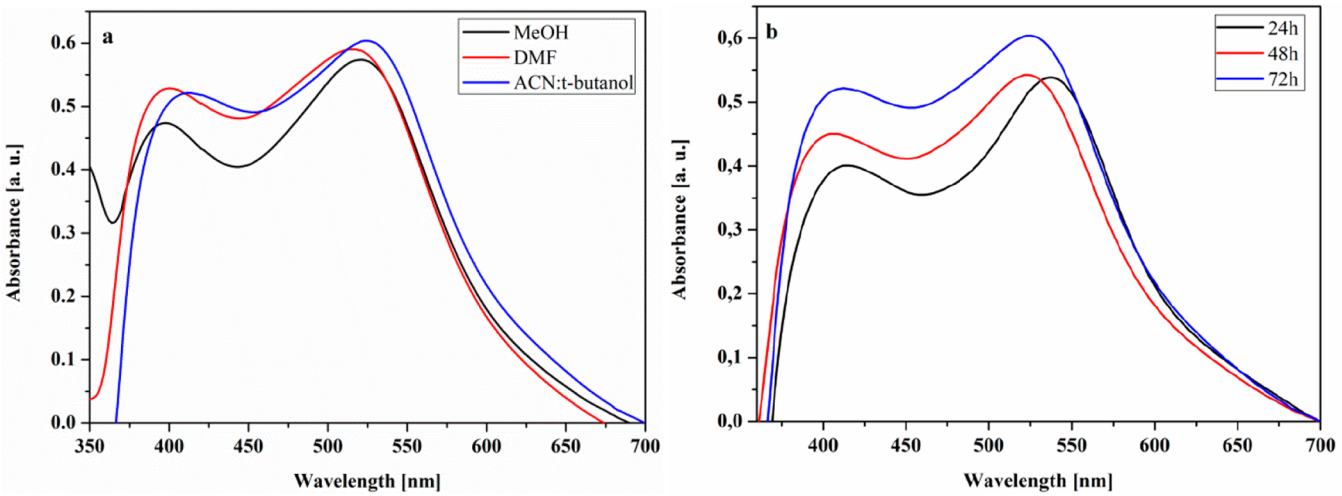

Figure 6. UV−vis spectra of photoanodes prepared in (a) various solvents after 72 h and (b) in ACN:*t*-BuOH (1:1) after 24, 48, and 72 h.

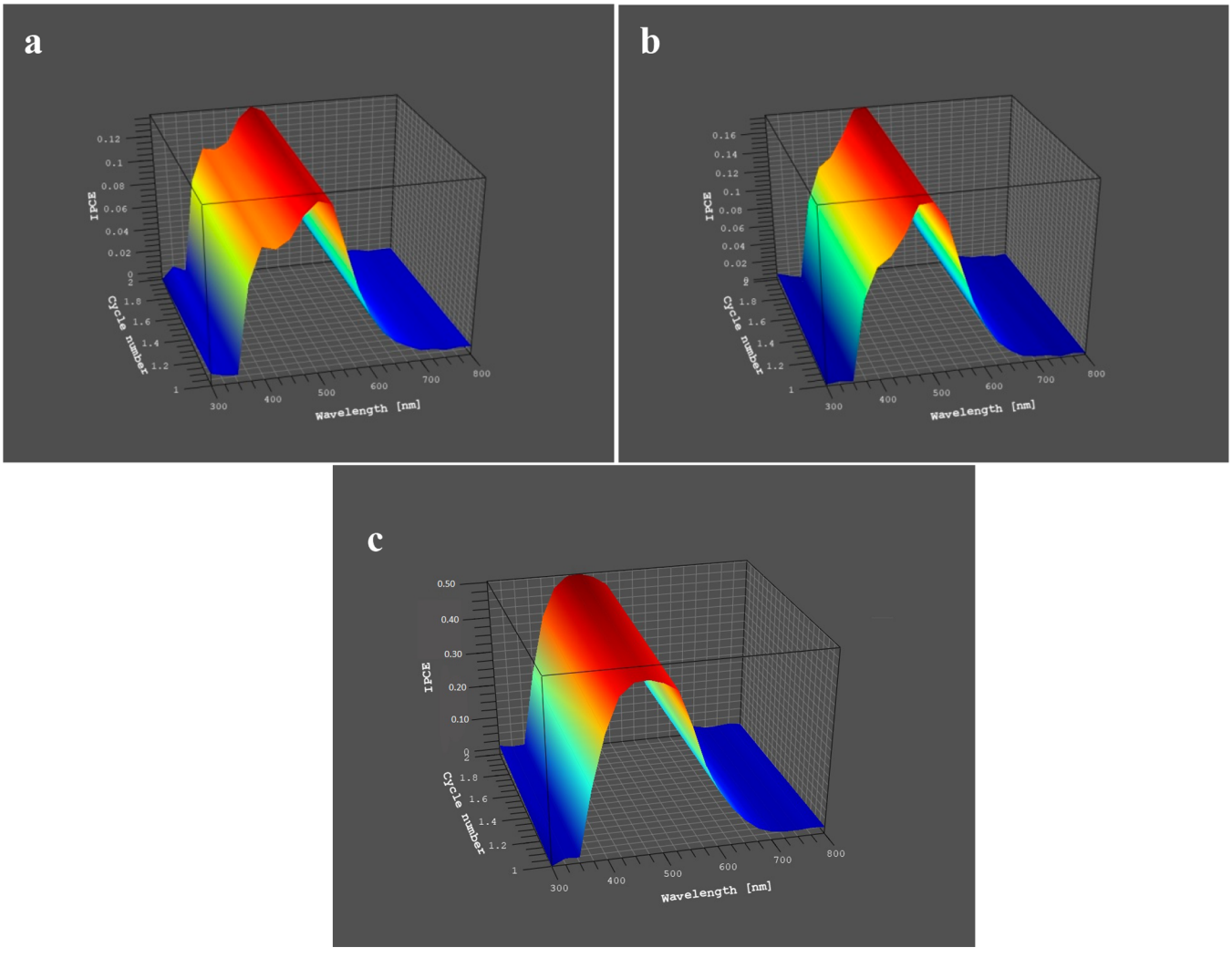

Figure 7. IPCE spectra of DSSCs consisting of photoanodes prepared in (a) MeOH, (b) DMF and (c) ACN:*t*-BuOH (72 h immersion time in solution).

reaction between solvents and the hydroxyl surface groups of TiO_2.[19] It was reported that the so-called donor number (DN) of a solvent is particularly important for the interaction between solvent and the TiO_2 hydroxyl groups. The donor number is defined as the negative enthalpy of the complexation reaction of Lewis bases with the reference Lewis acid $SbCl_5$ in 1,2-dichloroethane.[54] The donor number of MeOH, DMF, ACN, and *t*-BuOH is 19, 26.6, 14.1, and 38 kcal mol^{-1},

https://dx.doi.org/10.1021/acs.energyfuels.0c02188
Energy Fuels 2020, 34, 14344−14355

Table 3. PV Data of Prepared Cells Collected from $J-V$ Curves and IPCE Spectra as Well as Adsorbed Dye Amount

solvent	time (h)	V_{oc} (mV)	J_{sc} (mA cm^{-2})	FF	PCE (%)	IPCE$_{max}$ (%)	$J_{sc\text{-}IPCE}$ (mA cm^{-2})	dye loading (mol cm^{-2})
MeOH	24	562	14.73	0.36	3.20			–
	48	628	18.45	0.45	5.05			–
	72	642	17.29	0.50	5.32	13	12.16	1.64×10^{-7}
DMF	24	664	12.22	0.55	4.45			–
	48	696	16.64	0.50	5.70			–
	72	719	17.96	0.48	6.24	17	11.95	2.26×10^{-7}
ACN:*t*-BuOH	24	730	13.19	0.56	5.46	–	–	–
	48	762	14.34	0.54	5.99	32	12.62	–
	72	696	21.34	0.41	6.30	50	12.33	2.95×10^{-7}

respectively.[55] Taking into account the interaction of chemical species, it could be concluded that solvents characterized by a higher DN (more Lewis basicity) interact forcefully with the TiO_2 surface, which is a Lewis acid. Thus, solvents with a higher DN value will cause more dye molecules to anchor to the TiO_2 surface.[19] The presented results indicate that, with increasing solvent DN value, the number of dye molecules anchored to the surface of TiO_2 increases. The most dye molecules were adsorbed using a mixture of ACN:*t*-BuOH (2.95×10^{-7} mol cm^{-2}) and the least were absorbed for MeOH (1.64×10^{-7} mol cm^{-2}). This translates directly into the current density value of the tested cells, which was also the highest for the solar cell prepared with ACN:*t*-BuOH (21.34 mA cm^{-2}) and the lowest for that prepared with MeOH (17.29 mA cm^{-2}).

To summarize, the best photovoltaic performance was exhibited by the solar cell with its photoanode prepared by adsorption of dye from ACN:*t*-BuOH during 72 h (Figure 8.

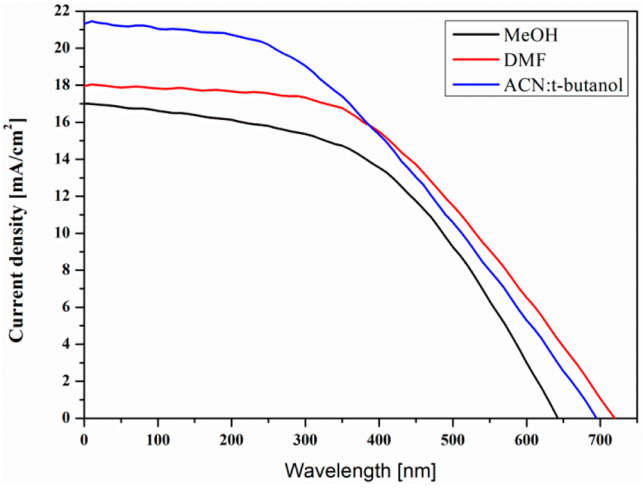

Figure 8. Photocurrent density–voltage curves ($J-V$) of DSSCs with their photoanode prepared using various solvents (72 h immersion time).

3.3. Effect of Coadsorbents and Cosensitization. The role of coadsorbents is the reduction of the formation of dye aggregates onto the TiO_2 surface, which favors early recombination processes in devices, preventing high efficiencies.[24−27] However, it was found that the coadsorbent addition may or may not cause an improvement of photovoltaic performance of DSSCs, depending on the dye used. In this work, N719 dye solutions along with the coadsorbents cholic acid (CA), deoxycholic acid (DCA), and chenodeoxycholic acid (CDCA) ($c = 3 \times 10^{-4}$ M, coadsorbents $c = 10$ mM) were prepared. Usually, one of these coadsorbents is applied and the effect of its concentration on PV parameters of DSSCs is studied.[25,56,57] To the best of our knowledge, only in one article has the effect of the same coadsorbents (CA, DCA, and CDCA) but a different dye (SJW-E1) been reported.[25] It has been found that application of CA increased the device performance compared to cells with DCA and CDCA.

The UV–vis spectra of N719 adsorbed on TiO_2 in the presence of various coadsorbents are given in Figure 9.

With the addition of coadsorbents, the decrease of absorbance was observed and the highest drop was seen for the CDCA. The observed absorption reduction can be due to a decrease of the amount of adsorbed dye on the TiO_2 surface, which was confirmed by the desorption study (cf. Table 4).

As can be noted from Figure 10, which compares the IPCE spectra of TiO_2 exposed to N719 alone and to both dye and CDCA, the reached maximum value of IPCE was slightly higher in the presence of coadsorbent. Considering the relationship between the presence and type of coadsorbent and the PV response collected in Table 4, an improvement of the PCE in the case of CDCA addition, mainly due to a higher FF value, was seen. Thus, the results reflected the beneficial impact of CDCA on DSSC efficiency,[28] despite the fact that the coadsorbents differ only in the structure of the R substituents. However, to obtain a detailed explanation of the observed effect, investigations supported by density functional theory seem to be necessary, which are out of the scope of this work. In the literature, an explanation of the impact of the chemical structure of CA, DCA, and CDCA on DSSC performance has not been undertaken.

An approach to improve the DSSC's performance is mixing various dyes that have complementary absorption ranges or molar extinction coefficients to enhance the light-harvesting ability of the photoanode[58] or to reduce the device cost without sacrificing PV response.[59] In our previous work,[41] we presented the effect of mixing N719 with 5,5′-bis(2-cyano-1-acrylic acid)-2,2′-bithiophene (denoted as D-1 in Figure 1) on PV parameters. Herein, we extended the reported investigations by means of collecting the PV data of the devices after 1 year, utilizing a thinner TiO_2 layer (7.3 μm), and applying a mixture of N719 with D-1 and CDCA and a mixture of N719 with 2-cyano-3-(2,2′:5′,2″-terthiophen-5-yl)acrylic acid (D-2 in Figure 1). Figure 9b presents UV–vis spectra of a TiO_2 surface with adsorbed dyes. Comparison of the absorption bands indicates that mixing of two such dyes results in an increasing absorbance and absorption range in the case of the mixture of N719 and D-1. The UV–vis spectra also prove that molecules of two dyes on a TiO_2 substrate simultaneously adsorb radiation. The recorded IPCE spectra are depicted in Figure 10c,d, whereas the estimated PV parameters are

https://dx.doi.org/10.1021/acs.energyfuels.0c02188
Energy Fuels 2020, 34, 14344−14355

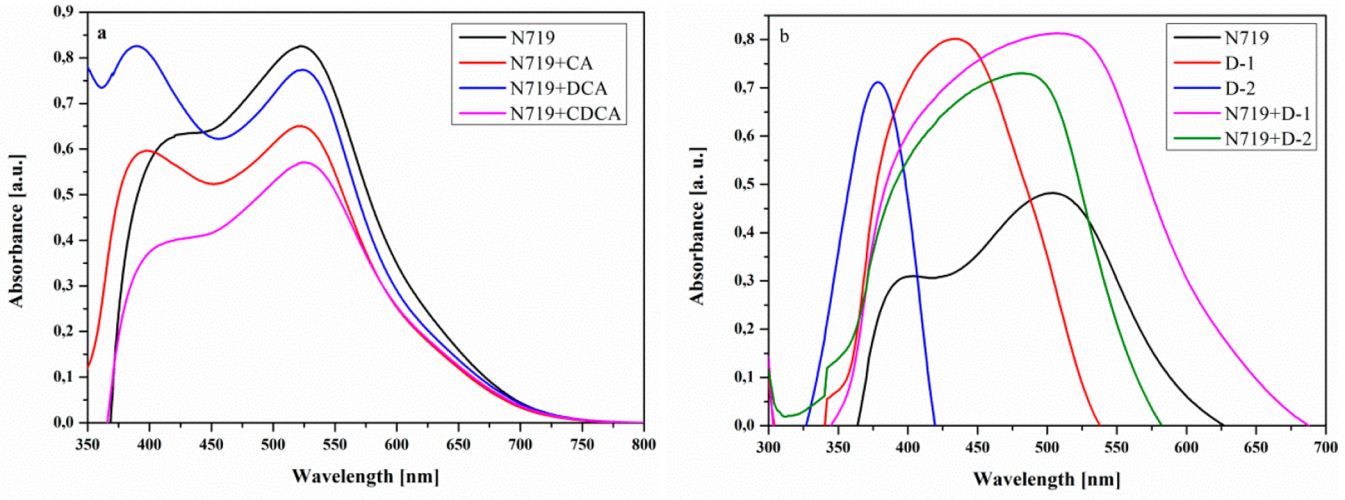

Figure 9. UV−vis absorption spectra of (a) N719 with and without coadsorbents and (b) with and without cosensitizers adsorbed on a 8.4 μm TiO_2 film.

Table 4. Effect of Addition of Coadsorbent and Cosensitizers on PV Parameters, IPCE Maximum, and Adsorbent Quantity

coadsorbent or dye	V_{oc} (mV)	J_{sc} (mA cm^{-2})	FF	PCE j(%)	IPCE (%)	$J_{sc\text{-}IPCE}$ (mA cm^{-2})	dye loading (mol cm^{-2})
w/o[a]	749	18.00	0.43	5.96	25	15.94	2.67×10^{-7}
CA[a]	758	14.31	0.52	5.82	23	15.37	–
DCA[a]	712	14.63	0.52	5.57	22	17.13	–
CDCA[a]	742	16.04	0.51	6.22	24	15.98	2.49×10^{-7}
D-1[b39]	366	0.55	0.43	0.14	–		–
D-2[b39]	285	0.72	0.44	0.09	–		–
N719[b39]	718	17.29	0.40	5.75	–		–
N719+D-1[b39]	655	20.98	0.45	6.30	–		–
N719[b] after 1 year	678	7.58	0.57	3.00	–		–
D-1[b] after 1 year	357	0.31	0.49	0.04	–		–
N719+D-1[b] after 1 year	630	9.96	0.49	3.15	–		–
N719[c]	696	16.54	0.49	5.67	16	11.88	–
N719+D-1[c]	646	21.00	0.45	6.22	23	12.34	–
N719+D-1+CDCA[c]	638	17.48	0.47	5.39	–		–
N719+D-2[c]	618	16.48	0.45	4.70	20	8.41	–

[a]Photoanode preparation conditions: TiO_2 thickness 8.4 μm, ACN:*t*-BuOH, 48 h, N719 $c = 3 \times 10^{-4}$ M, and coadsorbent $c = 10$ mM. [b]Photoanode preparation conditions: TiO_2 thickness 8.4 μm, DMF, 48 h, N719 $c = 3 \times 10^{-4}$ M. [c]Photoanode preparation conditions: TiO_2 thickness 7.3 μm, DMF, 48 h, N719 $c = 3$ x10^{-4} M.

collected in Table 4. Taking into account the effect of cosensitization by mixing N719 with dye D-1 (TiO_2 thickness 8.4 μm), a PCE improvement of about 0.5% in comparison to the device with N719 (alone) was seen.[41] However, as can be noted from Table 4, the utilization of D-2 as a cosensitizer caused a decrease of the PCE by almost 1%, mainly due to the lower value of V_{oc} (618 mV) compared to the reference cell based on N719 (696 mV). It is seen from the IPCE measurements that the device with a mixture N719 and D-2 exhibited a band in the region of 350−600 nm with a maximum value of 20%, while the cell based on solely N719 or on a mixture of N719 with D-1 showed a significantly broader band in the range of 350−700 nm. As a consequence of IPCE band extension, the low-energy electrons could be more effectively transmitted to the conduction band of TiO_2. Thus, although improvement of the PV response can be expected considering the UV−vis spectra of N719 with D-2 in comparison with that of neat N719 on TiO_2 (Figure 9b), in the end, the application of D-2 reduces the PCE value.

The next step of the investigation involved examination of coadsorbent application in the case of cosensitized (N719 with D-1) devices. The coadsorbent CDCA improved the PV performance of the device based on N719 when applied. However, contrary to expectations, the presence of CDCA significantly lowered the PCE value (from 6.22% to 5.39%) due to the less effective electron injection and lower dark current, as indicated by the lower J_{sc} (17.48 mA cm^{-2}) and V_{oc} (638 mV) in comparison to the cell without CDCA (J_{sc} = 21 mA cm^{-2}, V_{oc} = 646 mV).

As was mentioned in section 3.1, an anode consisting of two TiO_2 layers also seemed to be promising for DSSCs. Thus, to check the impact of TiO_2 thickness on cosensitized devices, cells based on N719 with D-1 and on neat N719 were fabricated. It was found that a DSSC with thinner TiO_2 (7.3 μm) showed practically the same PV response with insignificantly lower (about 0.08%) PCE compare to the device with 8.4 μm TiO_2 in the cases of N719 alone and a mixture of dyes (N719 with D-1).

https://dx.doi.org/10.1021/acs.energyfuels.0c02188
Energy Fuels 2020, 34, 14344−14355

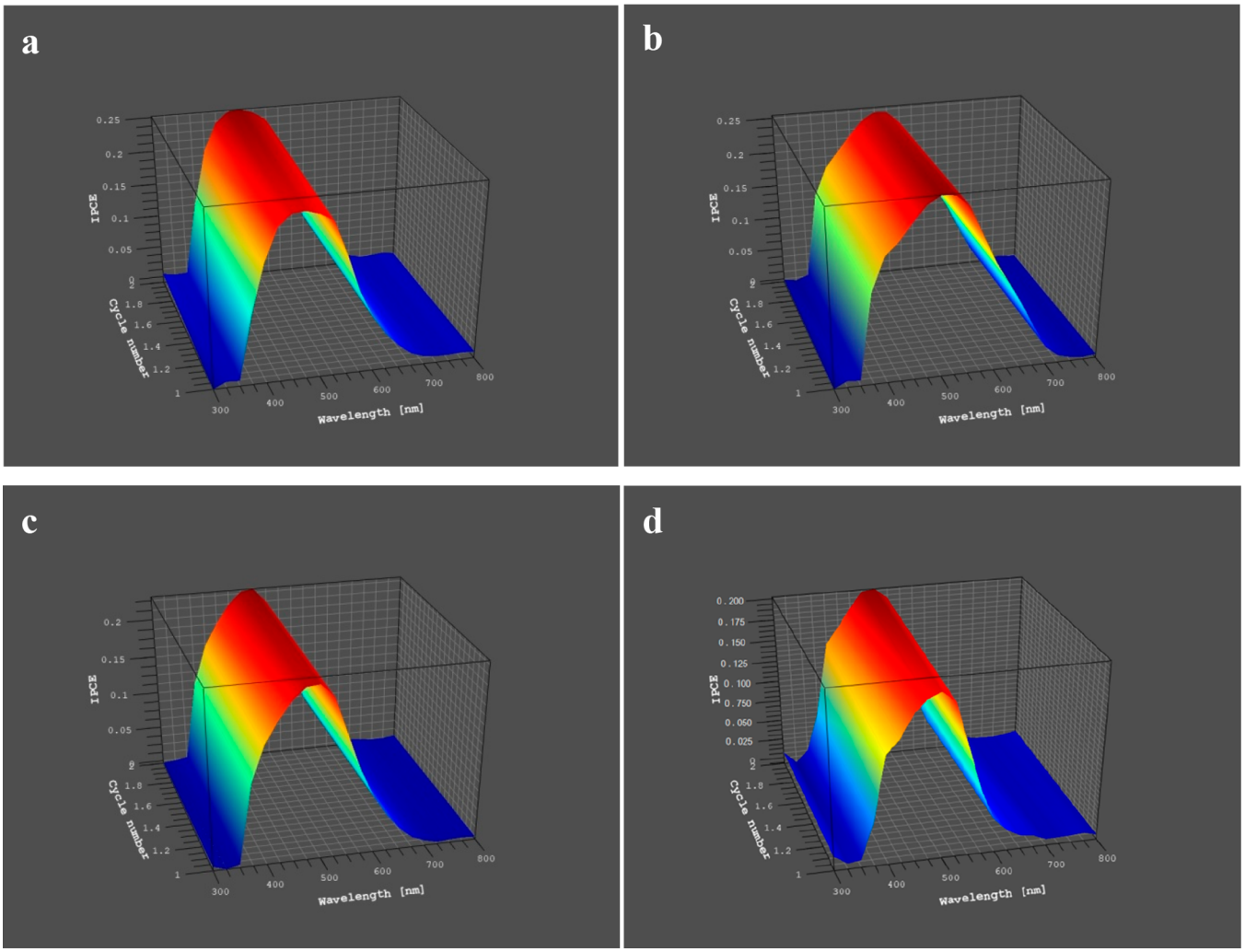

Figure 10. IPCE spectra of devices prepared from dye solutions (a) without and (b) with CDCA addition, sensitized with (c) N719+D-1 and (d) N719+D-2, for a TiO_2 thickness of 7.3 μm.

The long-term stability of a DSSC is crucial for practical applications. Thus, the $J-V$ characteristics of DSSCs with photoanodes consisting of 8.4 μm TiO_2 with adsorbed N719, D-1, and a mixture of dyes (N719, D-1) prepared 14 months ago were again measured. As can be seen from Table 4, the PCE values of unprotected devices cosensitized with N719 after time decreased to about 3%. However, it is worth noting that a solar cell containing a mixture of dyes (N719+D-1) still shows a higher efficiency (3.15%) than the reference device (3.00%). The observed drop in PV performance is mainly a result of significantly lowering the J_{sc} value. In the literature, there is a lack of information concerning the long-term stability of devices sensitized with N719.

4. CONCLUSIONS

The presented investigations were focused on the examination of photoanode fabrication, taking into account the thickness of the TiO_2 layer, the type of solvent used for dye solution preparation, the immersion time of the anode in the dye solution, and the addition of coadsorbents and cosensitizers, and determined the impact of those parameters on the photovoltaic response of DSSCs. A series of N719-sensitized solar cells was obtained. Two cyanoacrylic acid derivatives with thiophene units were applied as cosensitizers. From these investigations, the following conclusions can be made: (1) Devices with photoanodes consisting of two (thickness 7.3 μm) and four TiO_2 layers (15 μm) exhibited similar PCE values compared to a cell with three TiO_2 layers (thickness 8.4 μm). Thus, the preparation of thinner photoanodes could be justified from an economical point of view. (2) The PV response strongly depends on the nature of the solvent and the immersion time, and the performance order for the devices with photoanodes fabricated in different solvents was ACN:*t*-BuOH > DMF > MeOH. With an extension of immersion time from 24 to 48 h, an increase of the PCE in the range of 0.53%−1.85% was observed. The extension of time to 78 h resulted in a smaller PCE boost (0.27%−0.54%) in relation to 48 h. The lowest changes in the PCE for various immersion times were found for ACN:*t*-BuOH. (3) Utilization of chenodeoxycholic acid as a coadsorbent with N719 resulted in improvement of the PCE value (6.22%) relative to the reference device (5.96%), in contrast to results with cholic acid and deoxycholic acid. However, addition of CDCA in the case of a cosensitized device (N719+D-1) did not improved the PV parameters, and even decreased the PV performance. (4) The idea of cosensitization was effective in the case of applying 5,5′-bis(2-cyano-1-acrylic acid)-2,2′-bithiophene, which raised the PCE about 0.55%, together with decreasing by half the amount

https://dx.doi.org/10.1021/acs.energyfuels.0c02188
Energy Fuels 2020, 34, 14344−14355

of N719. (5) The examination of the long-term stability of unprotected photoanode examined after 14 months showed a drop in the PCE of about 2.75% and 3.15% for the device based on N719 and on a mixture N719 with D-1, respectively.

AUTHOR INFORMATION

Corresponding Author

Ewa Schab-Balcerzak − *Centre of Polymer and Carbon Materials, Polish Academy of Sciences, 41-819 Zabrze, Poland; Institute of Chemistry, University of Silesia, 40-006 Katowice, Poland;* orcid.org/0000-0002-7219-8664; Email: ewa.schab-balcerzak@us.edu.pl

Authors

Paweł Gnida − *Centre of Polymer and Carbon Materials, Polish Academy of Sciences, 41-819 Zabrze, Poland;* orcid.org/0000-0003-3350-9383

Marcin Libera − *Institute of Chemistry, University of Silesia, 40-006 Katowice, Poland*

Agnieszka Pająk − *Institute of Chemistry, University of Silesia, 40-006 Katowice, Poland*

Complete contact information is available at: https://pubs.acs.org/10.1021/acs.energyfuels.0c02188

Notes

The authors declare no competing financial interest.

ACKNOWLEDGMENTS

This work was supported by the National Science Centre of Poland (Grant No. 2016/23/B/ST8/02045).

REFERENCES

(1) Shakeel Ahmad, M.; Pandey, A. K.; Abd Rahim, N. *Advancements in the development of TiO_2 photoanodes and its fabrication methods for dye sensitized solar cell (DSSC) applications. A review Renew. Renewable Sustainable Energy Rev.* **2017**, *77*, 89−108.

(2) Breyer, C.; Bogdanov, D.; Aghahosseini, A.; Gulagi, A.; Child, M.; Oyewo, A. S.; Farfan, J.; Sadovskaia, K.; Vainikka, P. Solar photovoltaics demand for the global energy transition in the power sector. *Prog. Photovoltaics* **2018**, *26*, 505−523.

(3) Johnson, N. M.; Smolin, Y. Y.; Hagaman, D.; Soroush, M.; Lau, K. K. S.; Ji, H. F. Suitability of N-propanoic acid spiropyrans and spirooxazines for use as sensitizing dyes in dye-sensitized solar cells. *Phys. Chem. Chem. Phys.* **2017**, *19*, 2981−2989.

(4) Sivanadanam, J.; Mukkamala, R.; Mandal, S.; Vedarajan, R.; Matsumi, N.; Aidhen, I. S.; Ramanujam, K. Exploring the role of the spacers and acceptors on the triphenylamine-based dyes for dye-sensitized solar cells. *Int. J. Hydrogen Energy* **2018**, *43*, 4691−4705.

(5) Ashraf, S.; Yildirim, E.; Akhtar, J.; Siddiqi, H. M.; El-Shafei, A. *A comparative study of the influence of N, N′-dialkyl vs. N, N′-diaryl-based electron donor ancillary ligands on photocurrent and photovoltage in dye-sensitized solar cells (DSSCs) Phys. Phys. Chem. Chem. Phys.* **2017**, *19*, 20847−20860.

(6) Desta, M. B.; Vihn, N. S.; Kumar, C. P.; Chaurasia, S.; Wu, W.; Lin, J.; Wei, T.; Diau, E. W.-G. Pyrazine-incorporating panchromatic sensitizers for dye sensitized solar cells under one sun and dim light. *J. Mater. Chem. A* **2018**, *6*, 13778−13789.

(7) Lee, C. P.; Li, C. T.; Ho, K. C. Use of organic materials in dye-sensitized solar cells. *Mater. Today* **2017**, *20*, 267−283.

(8) Ye, M.; Wen, X.; Wang, M.; Iocozzia, J.; Zhang, N.; Lin, Ch; Lin, Z. Recent advances in dye-sensitized solar cells: from photoanodes, sensitizers and electrolytes to counter electrodes. *Mater. Today* **2015**, *18*, 155−162.

(9) Wang, W.; Xu, X.; Liu, Y.; Zhong, Y.; Shao, Z. Rational Design of Metal Oxide−Based Cathodes for Efficient Dye-Sensitized Solar Cells. *Adv. Energy Mater.* **2018**, *8*, 1800172.

(10) Kweon, D. H.; Baek, J.-B. Edge-Functionalized Graphene Nanoplatelets as Metal-Free Electrocatalysts for Dye-Sensitized Solar Cells. *Adv. Mater.* **2019**, *31*, 1804440.

(11) Smestad, G. P. Education and solar conversion: demonstrating electron transfer. *Sol. Energy Mater. Sol. Cells* **1998**, *55*, 157−178.

(12) Cha, S. I.; Kim, Y.; Hwang, K. H.; Shin, Y. J.; Seo, S. H.; Lee, D. Y. Dye-sensitized solar cells on glass paper: TCO-free highly bendable dye-sensitized solar cells inspired by the traditional Korean door structure. *Energy Environ. Sci.* **2012**, *5*, 6071−6075.

(13) Li, B.; Wang, L.; Kang, B.; Wang, P.; Qiu, Y. Review of recent progress in solid-state dye-sensitized solar cells. *Sol. Energy Mater. Sol. Cells* **2006**, *90*, 549−573.

(14) Wang, H.; Liu, G.; Li, X.; Xiang, P.; Ku, Z.; Rong, Y.; Xu, M.; Liu, L.; Hu, M.; Yang, Y.; Han, H. Highly efficient poly (3-hexylthiophene) based monolithic dye-sensitized solar cells with carbon counter electrode. *Energy Environ. Sci.* **2011**, *4*, 2025−2029.

(15) Yang, L.; Cappel, U. B.; Unger, E. L.; Karlsson, M.; Karlsson, K. M.; Gabrielsson, E.; Sun, L.; Boschloo, G.; Hagfeldt, A.; Johansson, E. M. J. Comparing spiro-OMeTAD and P3HT hole conductors in efficient solid state dye-sensitized solar cells. *Phys. Chem. Chem. Phys.* **2012**, *14*, 779−789.

(16) Agarwala, P.; Kabra, D. A review on triphenylamine (TPA) based organic hole transport materials (HTMs) for dye sensitized solar cells (DSSCs) and perovskite solar cells (PSCs): evolution and molecular engineering. *J. Mater. Chem. A* **2017**, *5*, 1348−1373.

(17) Zhang, J.; Yang, L.; Shen, Y.; Park, B.; Hao, Y.; Johansson, E. M. J.; Boschloo, G.; Kloo, L.; Gabrielsson, E.; Sun, L.; Jarboui, A.; Perruchot, Ch; Jouini, M.; Vlachopoulos, N.; Hagfeldt, A. Poly (3, 4-ethylenedioxythiophene) hole-transporting material generated by photoelectrochemical polymerization in aqueous and organic medium for all-solid-state dye-sensitized solar cells. *J. Phys. Chem. C* **2014**, *118* (30), 16591−16601.

(18) Suzuka, M.; Hayashi, N.; Sekiguchi, T.; Sumioka, K.; Takata, M.; Hayo, N.; Ikeda, H.; Oyaizu, K.; Nishide, H. A quasi-solid state DSSC with 10.1% efficiency through molecular design of the charge-separation and-transport. *Sci. Rep.* **2016**, *6*, 28022.

(19) Lee, K. M.; Suryanarayanan, V.; Ho, K. C. *Influences of different TiO_2 morphologies and solvents on the photovoltaic performance of dye-sensitized solar cells. J. Power Sources* **2009**, *188*, 635−641.

(20) Hamadanian, M.; Jabbari, V.; Gravand, A. *Dependence of energy conversion efficiency of dye-sensitized solar cells on the annealing temperature of TiO_2 nanoparticles. Mater. Sci. Semicond. Process.* **2012**, *15*, 371−379.

(21) Umale, S.; Sudhakar, V.; Sontakke, S. M.; Krishnamoorthy, K.; Pandit, A. B. *Improved efficiency of DSSC using combustion synthesized TiO_2. Mater. Res. Bull.* **2019**, *109*, 222−226.

(22) Ganesh, R. S.; Navaneethan, M.; Ponnusamy, S.; Muthamizhchelvan, C.; Kawasaki, S.; Shimura, Y.; Hayakawa, Y. *Enhanced photon collection of high surface area carbonate-doped mesoporous TiO_2 nanospheres in dye sensitized solar cells. Mater. Res. Bull.* **2018**, *101*, 353−362.

(23) Xi, J.; Dahoudi, N. A.; Zhang, Q.; Sun, Y.; Cao, G. *Effect of annealing temperature on the performances and electrochemical properties of TiO_2 dye-sensitized solar cells. Sci. Adv. Mater.* **2012**, *4*, 727−733.

(24) Lee, K. M.; Suryanarayanan, V.; Ho, K. C.; Justin Thomas, K. R.; Lin, J. T. Effects of co-adsorbate and additive on the performance of dye-sensitized solar cells: A photophysical study. *Sol. Energy Mater. Sol. Cells* **2007**, *91*, 1426−1431.

(25) Lee, K. M.; Wu, S.-J.; Chen, Ch-Y; Wu, Ch-G; Ikegami, M.; Miyoshi, K.; Miyasaka, T.; Ho, K-Ch Efficient and stable plastic dye-sensitized solar cells based on a high light-harvesting ruthenium sensitizer. *J. Mater. Chem.* **2009**, *19*, 5009−5015.

(26) Dhar, A.; Siva Kumar, N.; Asif, M.; Vekariya, R. L. Fabrication of D−π−A sensitizers based on different donors substituted with a dihydropyrrolo [3, 4-c] pyrrole-1, 4-dione bridge for DSSCs: influence of the CDCA co-absorbent. *New J. Chem.* **2018**, *42*, 12024−12031.

(27) Prakash, G.; Subramanian, K. Interaction of pyridine π-bridge-based poly(methacrylate) dyes for the fabrication of dye-sensitized

https://dx.doi.org/10.1021/acs.energyfuels.0c02188
Energy Fuels 2020, 34, 14344−14355

solar cells with the influence of different strength phenothiazine, fluorene and anthracene sensitizers as donor units with new anchoring mode. *New J. Chem.* **2018**, *42*, 17939−17949.
(28) Li, J.; Wu, W.; Yang, J.; Tang, J.; Long, Y.; Hua, J. Effect of chenodeoxycholic acid (CDCA) additive on phenothiazine dyes sensitized photovoltaic performance. *Sci. China: Chem.* **2011**, *54*, 699−706.
(29) Desai, N. D.; Khot, K. V.; Dongale, T.; Musselman, K. P.; Bhosale, P. N. *Development of dye sensitized TiO_2 thin films for efficient energy harvesting. J. Alloys Compd.* **2019**, *790*, 1001−1013.
(30) Zhang, Q.; Dandeneau, C. S.; Zhou, X.; Cao, C. ZnO nanostructures for dye-sensitized solar cells. *Adv. Mater.* **2009**, *21*, 4087−4108.
(31) Ko, S. H.; Lee, D.; Kang, H. W.; Nam, K. H.; Yeo, J. Y.; Hong, S. J.; Grigoropoulos, C. P.; Sung, H. J. Nanoforest of hydrothermally grown hierarchical ZnO nanowires for a high efficiency dye-sensitized solar cell. *Nano Lett.* **2011**, *11*, 666.
(32) Vittal, R.; Ho, K. C. Zinc oxide based dye-sensitized solar cells: A review. *Renewable Sustainable Energy Rev.* **2017**, *70*, 920−935.
(33) Rani, M.; Tripathi, S. K. *Electron transfer properties of organic dye sensitized ZnO and ZnO/TiO_2 photoanode for dye sensitized solar cells. Renewable Sustainable Energy Rev.* **2016**, *61*, 97−107.
(34) Aksoy, S.; Gorgun, K.; Caglar, Y.; Caglar, M. Effect of loading and standbye time of the organic dye N719 on the photovoltaic performance of ZnO based DSSC. *J. Mol. Struct.* **2019**, *1189*, 181−186.
(35) Rajan, A. K.; Cindrella, L. Ameliorating the photovoltaic conversion efficiency of ZnO nanorod based dye-sensitized solar cells by strontium doping. *Superlattices Microstruct.* **2019**, *128*, 14−22.
(36) Sinha, D.; De, D.; Goswami, D.; Mondal, A.; Ayaz, A. *ZnO and TiO_2 nanostructured dye sensitized solar photovoltaic cell* Mater. *Today Proc.* **2019**, *11*, 782−788.
(37) Kumara, N. T. R. N.; Ekanayake, P.; Lim, A.; Liew, L. Y. Ch.; Iskandar, M.; Ming, L. Ch.; Senadeera, G. K. R. Layered co-sensitization for enhancement of conversion efficiency of natural dye sensitized solar cells. *J. Alloys Compd.* **2013**, *581*, 186−191.
(38) Chen, Y.; Zeng, Z.; Li, C.; Wang, W.; Wang, X.; Zhang, B. *Highly efficient co-sensitization of nanocrystalline TiO_2 electrodes with plural organic dyes. New J. Chem.* **2005**, *29*, 773−776.
(39) Kimura, M.; Nomoto, H.; Masaki, N.; Mori, S. Dye molecules for simple co-sensitization process: Fabrication of mixed-dye-sensitized solar cells. *Angew. Chem.* **2012**, *124*, 4447−4450.
(40) Lee, K.; Lee, H.; Wang, D.; Park, N.; Lee, J.; Park, O.; Park, J. Dye-sensitized solar cells with Pt-and TCO-free counter electrodes. *Chem. Commun.* **2010**, *46*, 4505−4507.
(41) Kula, S.; Szlapa-Kula, A.; Fabianczyk, A.; Gnida, P.; Libera, M.; Bujak, K.; Siwy, M.; Schab-Balcerzak, E. Effect of thienyl units in cyanoacrylic acid derivatives toward dye-sensitized solar cells. *J. Photochem. Photobiol., B* **2019**, *197*, 111555.
(42) Chang, S.-M.; Lin, Ch-L; Chen, Y.-J.; Wang, H-Ch; Chang, W-Ch; Lin, L.-Y. Improved photovoltaic performances of dye-sensitized solar cells with ZnO films co-sensitized by metal-free organic sensitizer and N719 dye. *Org. Electron.* **2015**, *25*, 254−260.
(43) Uam, H.-S.; Jung, Y.-S.; Jun, Y.; Kim, K.-J. *Relation of Ru(II) dye desorption from TiO_2 film during illumination with photocurrent decrease of dye-sensitized solar cells. J. Photochem. Photobiol., A* **2010**, *212*, 122−128.
(44) Selvaraj, P.; Baig, H.; Mallick, T. K.; Siviter, J.; Montecucco, A.; Li, W.; Paul, M.; Sweet, T.; Gao, M.; Knox, A. R.; Sundaram, S. Enhancing the efficiency of transparent dye-sensitized solar cells using concentrated ligh. *Sol. Energy Mater. Sol. Cells* **2018**, *175*, 29−34.
(45) Marzec, A.; Pędzich, Z. Synteza nanokrystalicznych proszków TiO_2 o zróżnicowanych wielkościach cząstek i powierzchni właściwej metodą zol-żel (Preparation of TiO_2 nanocrystals with different particle size and specific surface area by the sol-gel method). *Materiały Ceramiczne (Ceramic Materials)* **2016**, *68.2*, 145−149 (ISSN 1996−1944)..
(46) Lin, F.-S.; Priyanka, P.; Fan, M.-S.; Vegiraju, S.; Ni, J.-S.; Wu, Y-Ch.; Li, Y.-H.; Lee, G.-H.; Ezhumalai, Y.; Jeng, R.-J.; Chen, M.-C.; Ho, K.-C. Metal-free efficient dye-sensitized solar cells based on thioalkylated bithiophenyl organic dyes. *J. Mater. Chem. C* **2020**, DOI: 10.1039/D0TC02310H.
(47) Kiran, S.; Naveen Kumar, S. K. *Preparation and Thickness Optimization of TiO_2/Nb_2O_5 Photoanode for Dye Sensitized Solar Cells. Mater. Today Proc.* **2018**, *5*, 10797−10804.
(48) Selvaraj, P.; Baig, H.; Mallick, T. K.; Siviter, J.; Montecucco, A.; Li, W.; Paul, M.; Sweet, T.; Gao, M.; Knox, A. R.; Sundaram, S. Enhancing the efficiency of transparent dye-sensitized solar cells using concentrated light. *Sol. Energy Mater. Sol. Cells* **2018**, *175*, 29−34.
(49) Suryanarayanan, V.; Lee, K.-M.; Chen, J.-G.; Ho, K-Ch High performance dye-sensitized solar cells containing 1-methyl-3-propyl imidazolinium iodide-effect of additives and solvents. *J. Electroanal. Chem.* **2009**, *633*, 146−152.
(50) Wu, J.; Lan, Z.; Lin, J.; Huang, M.; Li, P. Effect of solvents in liquid electrolyte on the photovoltaic performance of dye-sensitized solar cells. *J. Power Sources* **2007**, *173*, 585−591.
(51) Ghosh, S.; Sartape, R.; Chakraborty, J. Role of dye-induced corrosion in determining the efficiency of ZnO-based DSSC: the case of ZnO nanoforest in N719. *J. Mater. Sci.: Mater. Electron.* **2020**, *31*, 2202−2220.
(52) Sadikin, S. N.; Rahman, M. Y. A.; Umar, A. A. Zinc sulphide-coated titanium dioxide films as photoanode for dye-sensitized solar cells: Effect of immersion time on its performance. *Superlattices Microstruct.* **2019**, *130*, 153−159.
(53) Gaikwad, M. A.; Suryawanshi, M. P.; Nikam, S. S.; Bhosale, C. H.; Kim, J. H.; Moholkar, A. V. Influence of Zn concentration and dye adsorption time on the photovoltaic performance of M-SILAR deposited ZnO-based dye sensitized solar cells. *J. Photochem. Photobiol., A* **2016**, *329*, 246−254.
(54) Laurence, C.; Graton, J.; Gal, J. F. An overview of Lewis basicity and affinity scales. *J. Chem. Educ.* **2011**, *88*, 1651−1657.
(55) Cataldo, F. A revision of the Gutmann donor numbers of a series of phosphoramides including TEPA. *Eur. Chem. Bull.* **2015**, *4*, 92−97.
(56) Kumar, V.; Gupta, R.; Bansal, A. Role of chenodeoxycholic acid as co-additive in improving the efficiency of DSSCs. *Sol. Energy* **2020**, *196*, 589−596.
(57) Trilaksana, H.; Shearer, C.; Kloo, L.; Andersson, G. G. Restructuring of Dye Layers in Dye Sensitized Solar Cells: Cooperative Adsorption of N719 and Chenodeoxycholic Acid on Titania. *ACS Appl. Energy Mater.* **2019**, *2*, 124−130.
(58) Hemavathi, B.; Akash, S.; Kusuma, J.; Trupthi, C. D.; Shwetharani, R.; Balakrishna, R. G.; Shanmukappagouda; Ahipa, T. N. New 2-methoxy-4, 6-bis (4-(4-nitrostyryl) phenyl) nicotinonitrile: Synthesis, characterization and DSSC study. *J. Photochem. Photobiol., A* **2019**, *377*, 75−79.
(59) Kotowicz, S.; Sęk, D.; Kula, S.; Fabiańczyk, A.; Małecki, J. G.; Gnida, P.; Maćkowski, S.; Siwy, M.; Schab-Balcerzak, E. Photoelectrochemical and thermal characterization of aromatic hydrocarbons substituted with a dicyanovinyl unit. *Dyes Pigm.* **2020**, *180*, 108432.

https://dx.doi.org/10.1021/acs.energyfuels.0c02188
Energy Fuels 2020, 34, 14344−14355